

Intra- and Intermolecular Heavy-Atom Effects on the Fluorescence Properties of Brominated C₆₀ Polyads

M. Rae,[†] F. Perez-Balderas,[‡] C. Baleizão,[†] A. Fedorov,[†] J. A. S. Cavaleiro,[‡] A. C. Tomé,^{*,‡} and M. N. Berberan-Santos^{*,†}

Centro de Química-Física Molecular, Instituto Superior Técnico, 1049-001 Lisboa, Portugal, and Departamento de Química, Universidade de Aveiro, 3810-193 Aveiro, Portugal

Received: February 16, 2006; In Final Form: April 27, 2006

A series of brominated mono-methano[60]fullerene malonate derivatives (two diads and one triad) are investigated for intramolecular and external heavy-atom effects on their fluorescence. Significant internal and external heavy-atom effects are observed in the three cases. It is shown that the internal effect doubles when going from the diads to the triad. In bromobenzene and in iodobenzene, the external effect is predominant, and diads and triad behave identically.

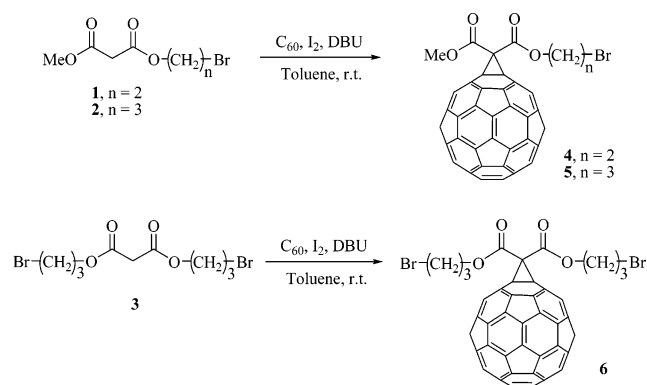
Introduction

The quenching of the fluorescence of fullerenes by the external heavy-atom effect^{1–3} has been the subject of several studies.^{4–6} It was established^{4,5} that, despite a very efficient intrinsic intersystem crossing (the intrinsic quantum yields of triplet formation being close to 1^{7–11}), fullerenes are still subject to the external heavy-atom effect that may significantly increase the intersystem crossing rate constant. For instance, whereas the fluorescence lifetime of a C₇₀ monoadduct in cyclohexane is 1.1 ns, in bromobenzene it drops to 400 ps, and in methyl iodide it is only 70 ps.⁴

A possible application of this effect in the case of the fullerenes is on their use as fast-responding optical limiters of intense laser pulses by reverse saturable absorption (RSA).^{4,12} In the case of fullerenes, RSA is based on triplet–triplet absorption and, therefore, occurs only after intersystem crossing. An increase in the intersystem crossing rate by the heavy-atom effect means a faster (picosecond) responding optical limiter, which is required for short laser pulses.⁴

Previous studies of the heavy-atom effect on the fluorescence of fullerenes^{4–6} dealt exclusively with the external (intermolecular) effect. In the case of C₇₀ and one monoadduct of C₇₀, it was concluded that the quenching was dynamic for several brominated and iodinated neutral quenchers. The Stern–Volmer plots obtained in hydrocarbon-quencher mixtures smoothly extrapolate to the results in pure liquid quencher solution, e.g., bromobenzene.⁴ The quenching was, in all cases, below diffusion control, and for this reason, (weak) fullerene fluorescence was still detected even in pure iodinated quenchers such as iodobenzene. The effect was, as expected, stronger in iodinated quenchers than in brominated ones.^{1,2,4} A detailed study⁶ of the heavy-atom effect in the case of C₇₀ and two different quenchers, iodide and bromobenzene, provided evidence for a quenching mechanism with exponential distance dependence. It was later shown that the recovered parameters for this mechanism (effective Bohr radius, quenching rate constant at contact) are

SCHEME 1: Bromoalkyl Methano[60]fullerene-dicarboxylates Synthesized



dependent on the radial distribution used for the quenchers.¹³ In the case of C₆₀ derivatives, including a water-soluble dendrimer,⁵ a quenching effect similar to that for C₇₀ and derivatives was observed for brominated and iodinated quenchers.

As mentioned, the internal heavy-atom effect on the fluorescence of fullerenes remains unexplored. In an interesting work, Weisman and co-workers¹⁴ investigated the effect of krypton in the endohedral fullerene Kr@C₆₀ on the excited state properties of the fullerene cage, but only triplet properties were measured.

In this work, we extend our previous studies of the heavy-atom effect on the fluorescence of fullerenes by investigating the intramolecular heavy-atom effect. For this purpose, the fluorophore F (a methano[60]fullerene-dicarboxylate) is covalently attached to one or two chains containing one bromine atom quencher (Q) at the end. Two different compounds (diads) of the FQ type and one compound (triad) of the FQ₂ type were synthesized (Scheme 1), and their fluorescence properties were determined. The use of the diad and polyad designations stems from the fact that, in these compounds, there are separated subunits that perform specific photophysical roles, in this case those of fluorophore and quencher. We also studied the effect of a supplementary external heavy-atom effect on the polyads by dissolving them in two heavy-atom solvents, bromobenzene and iodobenzene.

* To whom correspondence should be addressed. E-mail: actome@dq.ua.pt (A.C.T.); E-mail: berberan@ist.utl.pt, Fax: ++ 351 218464455, Tel: ++ 351 218419254 (M.N.B.S.).

[†] Instituto Superior Técnico.

[‡] Universidade de Aveiro.

Experimental Methods

Materials. High-purity C₆₀ and C₇₀ were purchased from Aldrich. Diethyl 1,2-methano[60]fullerene-61,61-dicarboxylate (DEM), used as a reference compound, was obtained from Fluka. All solvents used in the fluorescence studies were of spectroscopic grade.

Synthesis of the Bromoalkyl Methano[60]fullerene-dicarboxylates 4–6. The brominated C₆₀ fullerene diads **4** and **5** and triad **6** were prepared by cyclopropanation of C₆₀ with the corresponding malonate esters **1–3** (Scheme 1). The cyclopropanation reactions were carried out in toluene, in the presence of iodine and DBU (1,8-diazabicyclo[5.4.0]undec-7-ene), at room temperature, following a modification of the Bingel¹⁵ and Hirsch¹⁶ procedures. The compounds were characterized by ¹H and ¹³C NMR and mass spectrometry. The precursor malonate derivatives were prepared by reaction of the corresponding brominated alcohols with methyl 3-chloro-3-oxopropanoate (for derivatives **1** and **2**) or malonyl dichloride (for derivative **3**).

Synthesis of the Mixed Malonate Esters 1 and 2. A solution of methyl 3-chloro-3-oxopropanoate (200 μL, 2.0 mmol) in dichloromethane (10 mL) was added slowly to a dichloromethane (20 mL) solution of the required brominated alcohol (2.2 mmol) and NEt₃ (0.7 mL, 5 mmol) at 0 °C. After stirring at room temperature for 5 h, the reaction mixture was washed with a solution of 5% HCl (2 × 50 mL), then with a saturated solution of NaHCO₃ (2 × 50 mL), and at the end with water (50 mL). The organic phase was dried (Na₂SO₄), and the solvent was evaporated under reduced pressure. Compound **1**, 2-bromoethyl methyl malonate: 67% yield, ¹H NMR δ: 4.35 (t, *J* 6.1, 2H, OCH₂), 3.65 (s, 3H, CH₃O), 3.44 (t, *J* 6.1, 2H, CH₂Br), 3.35 (s, 2H, COCH₂CO); MS (EI) *m/z* 224, 226 (M⁺, 40%), 193, 195 [(M – CH₃O)⁺, 100%]. Compound **2**, 3-bromopropyl methyl malonate: 51% yield; ¹H NMR δ: 4.31 (t, *J* 6.0, 2H, OCH₂), 3.76 (s, 3H, CH₃O), 3.48 (t, *J* 6.5, 2H, CH₂Br), 3.41 (s, 2H, COCH₂CO), 2.20 (qui, *J* 6.2, 2H, CH₂CH₂CH₂); ¹³C NMR δ: 166.7, 166.1 (CO), 62.9 (CH₂O), 52.4 (CH₃O), 41.0 (COCH₂CO), 31.2 (CH₂CH₂CH₂), 29.0 (CH₂Br); MS (LSIMS) *m/z* 239, 241 (M + H)⁺.

Synthesis of the Symmetrical Malonate Ester 3, Bis(3-bromopropyl) Malonate. A solution of malonyl dichloride (200 μL, 2.0 mmol) in CH₂Cl₂ (10 mL) was added slowly to a CH₂Cl₂ (20 mL) solution of 3-bromopropan-1-ol (4.4 mmol) and NEt₃ (1.1 mL, 8 mmol) at 0 °C. After stirring at room temperature for 5 h, the reaction mixture was washed with a solution of 5% HCl (2 × 50 mL), then with a saturated solution of NaHCO₃ (2 × 50 mL), and at the end with water (50 mL). The organic phase was dried (Na₂SO₄), and the solvent was evaporated under reduced pressure. Compound **3**: 56% yield; ¹H NMR δ: 4.30 (t, *J* 6.0, 4H OCH₂), 3.48 (t, *J* 6.5, 4H, CH₂Br), 3.42 (s, 2H, CO–CH₂–CO), 2.21 (qui, *J* 6.3, 4H, CH₂CH₂–CH₂); ¹³C NMR δ: 165.9 (CO), 62.8 (OCH₂), 41.0 (COCH₂–CO), 31.0 (CH₂CH₂CH₂), 29.0 (CH₂Br); MS (LSIMS) *m/z* 345, 347, 349 (1:2:1) (M + H)⁺.

Synthesis of the Methano[60]fullerene-dicarboxylate Derivatives 4–6. To a solution of fullerene (80 mg, 0.11 mmol), malonate ester (0.13 mmol, 1.2 equiv), and iodine (0.13 mmol, 1.2 equiv) in toluene (50 mL) was added DBU (0.26 mmol, 2.4 equiv). After stirring for 6 h at room temperature, the solvent was removed under reduced pressure. The solid was redissolved in chloroform (25 mL) and filtered. Purification by flash chromatography, using cyclohexane/toluene (1:2) as eluent, afforded the desired product. Compound **4**, 2-bromoethyl methyl 1,2-methano[60]fullerene-61,61-dicarboxylate: 43% yield; *R_f* = 0.22 (cyclohexane:toluene 1:1); ¹H NMR δ: 4.82 (t, *J*

5.9, 2H, OCH₂), 4.13 (s, 3H, CH₃O), 3.72 (t, *J* 5.9, 2H, CH₂–Br); ¹³C NMR δ: 163.8 and 163.4 (CO), 145.3, 145.2, 145.1, 145.0, 144.9, 144.8, 144.7, 143.9, 143.0, 142.2, 141.9, 141.0, 66.3, 54.2, 27.9 (CH₂Br); MS (LSIMS) *m/z* 942, 994 (M⁺). Compound **5**, 3-bromopropyl methyl 1,2-methano[60]fullerene-61,61-dicarboxylate: 28% yield (81% based on the consumed C₆₀); *R_f* = 0.31 (cyclohexane:toluene 1:1); ¹H NMR δ: 4.67 (t, *J* 5.9, 2H, OCH₂), 4.11 (s, 3H, CH₃O), 3.58 (t, *J* 6.4, 2H, CH₂Br), 2.40 (m, 2H, CH₂CH₂CH₂); MS (LSIMS) *m/z* 957, 959 (M + H)⁺. Compound **6**, bis(3-bromopropyl) 1,2-methano[60]fullerene-61,61-dicarboxylate: 48% yield (70% yield based on the consumed C₆₀); *R_f* = 0.44 (cyclohexane:toluene 1:1); ¹H NMR δ: 4.67 (t, *J* 6.0, 4H, OCH₂), 3.58 (t, *J* 6.4, 4H, CH₂Br), 2.41 (qui, *J* 6.2, 4H, CH₂CH₂CH₂); ¹³C NMR δ: 163.4 (CO), 145.3, 145.2, 145.0, 144.93, 144.89, 144.70, 144.68, 144.6, 143.9, 143.1, 143.04, 143.00, 142.2, 141.9, 141.0, 139.0, 129.0, 128.2, 71.3, 65.0, 51.8, 31.3, 29.0 (CH₂Br); MS (LSIMS) *m/z* 1065, 1066, 1067 (M + H)⁺.

Spectroscopic Measurements. ¹H and ¹³C NMR spectra were recorded on a Bruker AMX 300 spectrometer at 300.13 and 75.47 MHz, respectively. CDCl₃ was used as solvent and tetramethylsilane as internal reference; the chemical shifts are expressed in δ (ppm), and the coupling constants (*J*) are in Hz. Mass spectra were recorded on a VG AutoSpec Q mass spectrometer using chloroform as the solvent and NBA as the matrix. Flash chromatography was carried out in silica gel (Fluka, 230–400 mesh). Electronic absorption spectra were recorded on a Shimadzu Model 3101 UV–vis–NIR spectrometer and emission spectra on a Spex Fluorolog F112A fluorimeter. The fluorescence quantum yields were determined from instrument-corrected spectra using C₇₀ and C₆₀ in toluene as standards ($\Phi_F = 5.7 \times 10^{-4}$ and $\Phi_F = 3.2 \times 10^{-4}$, respectively⁸). For fluorescence spectra, the instrumental bandwidths used were 18 nm in excitation and 16 nm in emission. All solutions used had an absorbance of 0.1 or lower for the steady-state measurements. Time-resolved picosecond fluorescence measurements were performed using the single-photon counting timing method with laser excitation. The setup consisted of a mode-locked Coherent Innova 400–10 argon ion laser that synchronously pumped a cavity dumped 710–2 dye (Rhodamine 6G) laser, delivering 3–4 ps pulses (with ca. 40 nJ/pulse) at a frequency of 3.4 MHz. In addition, a Ti:sapphire laser, constructed in our laboratory, was used. The experimental layout consists of a diode-pumped solid-state Nd:YVO₄ laser (Spectra Physics Millennia Xs) that pumps the self-mode-locked cavity dumped Ti:Sapphire laser. Typical duration of 60 nJ pulses, dumped at a repetition rate up to 2 MHz, is measured to be ca. 80 fs. The wavelength of the Ti:Sapphire laser can be changed from 750 to 860 nm. The output of the cavity dumped laser is frequency doubled with a 1.5 mm LBO crystal with efficiency ca. 40% and tripled with a 0.8 mm BBO crystal with ca. 15% efficiency. Intensity decay measurements were made by an alternate collection of impulse and decay, with the emission polarizer set at the magic angle position. Impulse was recorded slightly away from the excitation wavelength with a scattering suspension. For the decays, a cutoff filter was used, effectively removing all excitation light. The emission signal was passed through a depolarizer, a Jobin-Yvon HR320 monochromator with a grating of 100 lines/nm and was recorded on a Hamamatsu 2809U-01 microchannel plate photomultiplier as a detector. Time scales of 3.5–10 ps/channel were used for the monoderivatives in THF, of 3.0 ps/channel for the monoderivatives in bromobenzene, and of 1.3 ps/channel for the monoderivatives in iodobenzene. The instrument response function

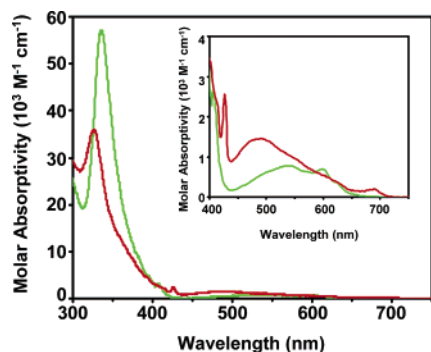


Figure 1. Comparison between the absorption spectrum of the methano[60]fullerene-dicarboxylates (red lines, in THF) and the absorption spectrum of C₆₀ (green lines, in toluene). (Inset) Weak transitions in the visible region.

TABLE 1: Absorption Spectral Features

compound	solvent	abs max (nm)
C ₆₀	toluene	406, 535
DEM	THF	426, 489, 690
4	THF	426, 472, 689
5	THF	426, 487, 693
6	THF	426, 490, 691

had an effective fwhm of 35 picoseconds. Usually, no less than 5000 counts were accumulated at the maximum channel.

Results and Discussion

Absorption and Fluorescence Spectra. Monofunctionalization brings a slight reduction to the cage π -electronic system and also a lowering of the cage symmetry, and as a result, the [60]fullerene derivatives exhibit photophysical properties not identical to those of C₆₀. Previous studies^{8,17} have shown that for monofunctionalized C₆₀ derivatives, a higher number of transitions in the absorption spectrum are observed, along with a slight increase in the fluorescence lifetime and a substantial increase in the fluorescence quantum yield. The photophysics of monofunctionalized derivatives of C₆₀ remain nevertheless characterized by exceedingly slow radiative transitions and a very fast intersystem crossing; accordingly, [60]fullerene mono-derivatives are still weakly fluorescent.

All methanofullerenes studied have similar absorption and fluorescence spectra. The absorption spectra of the methano-[60]fullerene-dicarboxylates in THF and of C₆₀ in toluene are shown in Figure 1. The inset displays the weak transitions in the visible region. The common absorption spectrum of the methano[60]fullerene-dicarboxylates is clearly different from that of C₆₀ in toluene in the visible region, with the following main distinctive features: (i) a significant red-shift of the C₆₀ 406 nm sharp absorption band to 426 nm in all cases; (ii) a significant (50–60 nm) blue-shift of the C₆₀ broad absorption band in the visible (maximum at 535 nm), see Table 1; (iii) the appearance of a new weak band at ca. 688 nm. This last feature is characteristic of monoaddition.^{8,17} The spectra of the derivatives in toluene do not show significant shifts with respect to those in THF. Like other C₆₀ monofunctionalized derivatives, the studied mono-methanoderivatives are stronger absorbers in the visible region than C₆₀, as a result of the cage symmetry reduction.

The fluorescence spectrum of the methano[60]fullerene-dicarboxylates is shown in Figure 2. The different addends do not significantly affect it. The fluorescence peak maxima occur at approximately the same emission wavelength as for C₆₀. However, whereas in the C₆₀ case the maximum corresponds

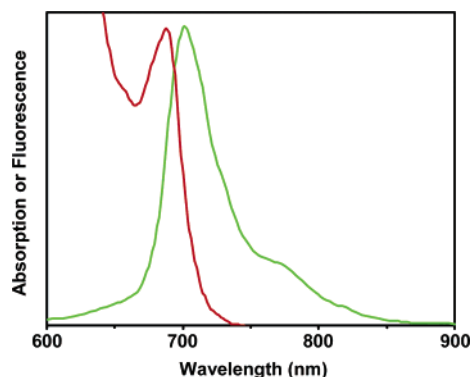


Figure 2. Electronic absorption spectrum (red) and fluorescence spectrum (green) of the methano[60]fullerene-dicarboxylates in THF, displaying the mirror image relationship.

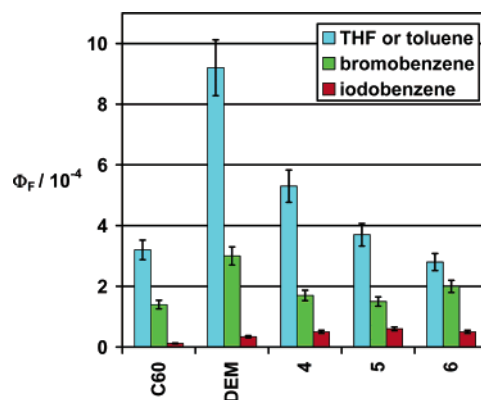


Figure 3. Fluorescence quantum yields of C₆₀ and of the C₆₀ derivatives.

TABLE 2: Fluorescence Quantum Yields

compound	$\Phi_F/10^{-4}$		
	toluene or THF	bromobenzene	iodobenzene
C ₆₀	3.2	1.4	0.12
DEM	9.2	3.0	0.34
4	5.3	1.7	0.5
5	3.7	1.5	0.6
6	2.8	2.0	0.5

to a higher vibronic transition, in the derivatives it corresponds to the 0–0 band, and a Franck–Condon progression typical of a small geometry change between the ground and excited states is clearly observed. A good mirror image of the fluorescence and absorption of the C₆₀ derivatives is observed (see Figure 2), with a small Stokes shift of 11–14 nm.

Fluorescence Quantum Yields. The fluorescence quantum yields (Φ_F) of the methano[60]fullerene derivatives were measured in THF and also in bromobenzene and iodobenzene. The value for C₆₀ refers to toluene, as it is insoluble in THF. The diethyl methano[60]fullerene-dicarboxylate has identical quantum yields in THF and in toluene, which coincide (within experimental error) with the measured value in chloroform,¹⁷ 1.0×10^{-3} . The values are graphically summarized in Figure 3 and are also given in Table 2. Several conclusions can be drawn from Figure 3: (i) The substantial increase in the quantum yield upon addition, i.e., when going from C₆₀ to the diethyl dicarboxylate; (ii) It is clear that this increase is no longer observed for the bromoalkyl derivatives, whose quantum yields in THF are similar to that of C₆₀. This is a direct evidence of an internal heavy-atom quenching effect; (iii) In THF, significant differences are observed between the 4/5 pair and 6, i.e., between monobrominated diads and the dibrominated triad, with the

dibrominated one experiencing the stronger internal effect; (iv) In bromobenzene, all quantum yields decrease significantly and become comparable; (v) A further decrease occurs in iodobenzene; all quantum yields are again comparable, with the exception of that of C₆₀, which is distinctly lower. The external heavy-atom effect thus follows the expected order and dominates over the internal one both in bromobenzene and in iodobenzene.

Fluorescence Decay of the Polyads. The fluorescence decay law of the fullerene moiety in a polyad, $I(t)$, is given by the general equation¹⁸

$$I(t) = \exp(-t/\tau_0) \exp(-\int_0^t k(u)du) \quad (1)$$

where τ_0 is the intrinsic fluorescence lifetime, and the time-dependent rate coefficient $k(t)$ is

$$k(t) = \int_0^\infty N(r,t)k(r)dr \quad (2)$$

and $N(r,t)$ is the number of quenchers at a distance r at time t . Note that eq 1 implies an assumption of additivity of contributions from different quenchers. It is also implicitly assumed in eq 1 that the intrinsic fluorescence lifetime is the same, irrespective of the distance between fluorophore and quencher. This assumption is a reasonable one for fluorescence. In the case of heavy-atom quenching, the quenching rate constant falls exponentially with the distance,⁶

$$k(r) = \frac{1}{\tau_0} \exp\left[-\frac{2(R_0 - r)}{L}\right] \quad (3)$$

where L is the effective Bohr radius, with typical values between 1 and 2 Å, and R_0 is the critical radius,⁶ with values typically smaller than 10 Å. For the pair C₇₀-bromobenzene, the estimated values for these parameters are⁶ $L = 2.6$ Å and $R_0 = 5.4$ Å.

In a fluid medium, $N(r,t)$ is obtained from an appropriate diffusion equation. However, the *rapid diffusion* limit suffices for our purposes. This limit is fulfilled in liquid solutions at room temperature for low quenching efficiencies. In such a case, $N(r,t)$ is time-independent and constantly equal to the equilibrium value $N(r) = N(r,0)$, and the decay is thus exponential.

In the intramolecular quenching case,

$$N(r) = Nf_i(r) \quad (4)$$

where $N_i = 1$ for the diads and $N_i = 2$ for the triad, and $f_i(r)$ is the distance distribution function for a covalently linked (intramolecular) fluorophore-quencher pair. It follows that

$$k_i = N_i \int_0^\infty f_i(r)k(r)dr \quad (5)$$

and if $f_i(r)$ is the same for the diad and for the triad, one expects a doubling of the quenching rate constant when going from the diad to the triad, in accordance with the starting assumption of additivity of contributions from different quenchers.

In the case of an additional quenching by the solvent, an intermolecular term must be added to the overall quenching rate constant,

$$k = k_i + k_e \quad (6)$$

where k_e is the rate constant for the quenching by the solvent. This rate constant can be written again in the form of eq 5,

$$k_e = \int_0^\infty N_e(r)k(r)dr \quad (7)$$

where

$$N_e(r) = Nf_e(r) = N_A[Q]4\pi r^2 g(r) \quad (8)$$

and where $f_e(r)$ is the distance distribution function for an intermolecular fluorophore-quencher pair, $g(r)$ is the radial distribution function,¹³ and $[Q]$ is the external quencher (solvent) concentration.

Using eq 8, the rate constant for external quenching becomes

$$k_e = N_A[Q] \int_0^\infty 4\pi r^2 g(r)k(r)dr = k_q[Q] \quad (9)$$

where k_q is the bimolecular rate constant for quenching. Assuming that the radial distribution function is a step function, i.e., that the quenchers are randomly and independently distributed around the excited molecule,

$$g(r) = \begin{cases} 0 & \text{if } r < d \\ 1 & \text{if } r > d \end{cases} \quad (10)$$

where d is the distance of closest approach, one obtains from eqs 3 and 9 that the bimolecular quenching rate constant is^{6,19}

$$k_q = \frac{\pi N_A L^3}{\tau_0} \left[1 + 2\frac{d}{L} + 2\left(\frac{d}{L}\right)^2 \right] \exp\left[-\frac{2(R_0 - d)}{L}\right] \quad (11)$$

For a general $g(r)$, the bimolecular quenching rate constant can only be obtained numerically.¹³

When $k_e \gg k_i$, intermolecular quenching is the dominant contribution and all polyads display similar photophysical behavior, irrespective of N_i .

For a given heavy-atom quenching moiety, and for the purposes of comparison with intermolecular quenching (e.g., polyad with a brominated moiety versus brominated solvent), eq 5 can be rewritten as

$$k_i = k_q[Q]_{\text{eff}} \quad (12)$$

where k_q is the rate constant for intermolecular quenching and $[Q]_{\text{eff}}$ is an effective quencher concentration defined by eq 12.

Fluorescence Lifetimes. For C₆₀ and monofunctionalized derivatives, the lifetime is controlled by the nonradiative decay constant, which in turn is practically identical to the intersystem crossing rate constant. In this way, the measured lifetimes directly reflect the enhanced intersystem crossing by the heavy-atom effect, when it exists. The fluorescence lifetimes of the studied methano[60]fullerene derivatives were measured in THF, bromobenzene, and iodobenzene. The value for C₆₀ (1.1 ns) refers again to toluene, as C₆₀ is insoluble in THF. The diethyl methano[60]fullerene-dicarboxylate has similar lifetimes in THF (1.4 ns) and in toluene (1.5 ns). The values are graphically summarized in Figure 4 and are also given in Table 3. The following conclusions can be drawn from Figure 4: (i) The increase in the lifetime upon addition of a group to the fullerene cage, i.e., when going from C₆₀ to the diethyl dicarboxylate, is moderate; (ii) This increase is no longer observed for the brominated derivatives, whose lifetimes in THF are on the contrary lower than that of C₆₀, and also lower than the lifetime of the reference compound, DEM. This is again direct evidence of an internal heavy-atom quenching effect; (iii) Within experimental error, no significant difference is observed between diads **4** and **5**, which differ in the chain length by one methylene group; (iv) Significant differences are observed in THF between

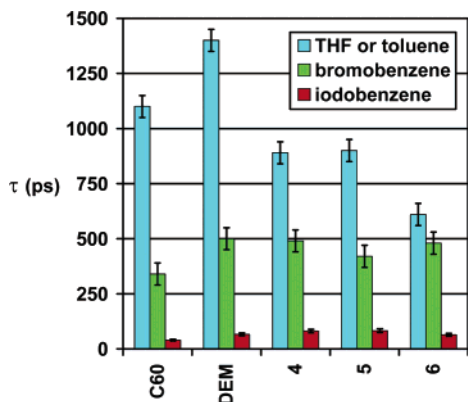


Figure 4. Fluorescence lifetimes of C₆₀ and of the C₆₀ derivatives.

TABLE 3: Fluorescence Lifetimes

compound	τ (ns)		
	toluene or THF	bromobenzene	iodobenzene
C ₆₀	1.1	0.34	0.040
DEM	1.4	0.50	0.066
4	0.89	0.49	0.081
5	0.90	0.42	0.083
6	0.61	0.48	0.064

the diads (4 and 5) and the triad 6, i.e., between the monobrominated derivatives and the dibrominated derivative, with the triad experiencing the stronger internal effect; (v) In bromobenzene all lifetimes decrease significantly, and become comparable, with values close to 500 ps, with the exception of that of C₆₀, 340 ps, which is distinctly lower; (vi) A further major decrease occurs in iodobenzene; all lifetimes are again comparable, with values between 64 and 83 ps, with the exception of that of C₆₀, 40 ps, which is distinctly lower. The external heavy-atom effect thus follows the expected order and dominates over the internal one both in bromobenzene and in iodobenzene. These conclusions are in agreement with those reached from the quantum yield data.

Internal vs External Heavy-Atom Effect. To compare the relative efficiency of internal and external (bromobenzene) heavy-atom effects, an effective concentration of quenchers, $[Q]_{\text{eff}}$, was computed for the intramolecular (internal) effect, see eq 12.

As mentioned in the Introduction, the intermolecular quenching processes in the case of C₇₀ and derivatives,⁴ and a C₆₀ derivative,⁵ were all found to be dynamic (straight Stern–Volmer plot with a common slope for intensities and lifetimes) and well below diffusion control for brominated quenchers. Taking the lifetime of DEM in THF (see Table 3) as the reference value, and using the previously measured⁵ bimolecular rate constant for the quenching of DEM by bromobenzene, $(1.9 \pm 0.4) \times 10^8 \text{ M}^{-1} \text{ s}^{-1}$, and using the lifetimes of the C₆₀ derivatives measured in THF (Table 3), the following effective quencher concentrations are obtained from the Stern–Volmer equation, see also Figure 5: 2.2 M (4), 2.1 M (5), and 4.9 M (6). Note that the concentration of neat bromobenzene is 9.52 M. The effective concentrations computed appear to be acceptable, given all approximations made. For the diads 4 and 5, the effective concentrations coincide within experimental error, as expected. The value corresponds to one bromine atom in a shell with a thickness of 1.6 Å around the fullerene cage (radius 5.3 Å), which is not unreasonable given the short range of the heavy-atom interaction⁶ and the fact that the chain restricts the mobility of the bromine atom. When going from the diads 4

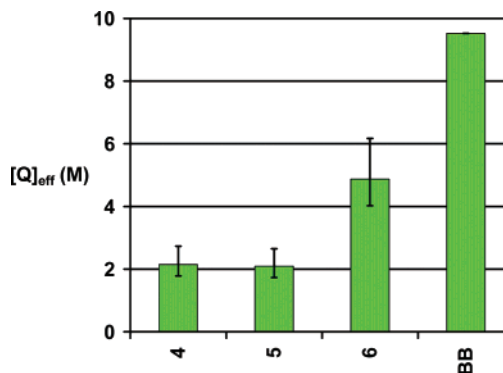


Figure 5. Effective concentration of the brominated moiety for the diads and triad and for the reference molecule (BB: bromobenzene). Error bars reflect the uncertainty in the value of the quenching rate constant of DEM by bromobenzene.

and 5 to the dibrominated triad 6, the effective concentration of quenchers approximately doubles, as expected.

Conclusions

The bromoalkyl methano[60]fullerene-dicarboxylates studied do exhibit an internal heavy-atom effect, with the effective quencher concentration doubling when going from the diads to the triad. A corresponding reduction of the fluorescence lifetimes is observed, which are lower than those of both the pristine C₆₀ and the nonbrominated diethyl dicarboxylate derivative.

A significant external heavy-atom effect is observed in bromobenzene and in iodobenzene. In bromobenzene, all quantum yields and lifetimes decrease significantly and become comparable, as expected for molecules containing the same fluorophore (DEM, 4, 5, and 6) and subject to the same quencher. A further strong decrease occurs in iodobenzene. All quantum yields and lifetimes are again comparable. Despite having a shorter intrinsic lifetime, C₆₀ has distinctly lower lifetimes in both solvents when compared to the studied derivatives, showing that it is subject to a stronger quenching effect. The external heavy-atom effect follows the expected halogen order, with the iodinated quencher being more effective than the brominated one. The external effect is found to largely surpass the internal one both in bromobenzene and in iodobenzene. With respect to bromobenzene, this is compatible with the higher concentration of quenchers, compared to the effective concentration of the brominated moiety in the intramolecular case. In the case of iodobenzene, this is explained by both the higher concentration of quenchers and the higher quenching efficiency of iodine.

Acknowledgment. This work was supported by Fundação para a Ciência e a Tecnologia (FCT, Portugal) and POCI 2010 (FEDER) within projects POCI/QUI/58515/2004 and POCI/QUI/58535/2004. C. Baleizão was supported by a postdoctoral fellowship from FCT (SFRH/BPD/14561/2003).

References and Notes

- (1) Birks, J. B. *Photophysics of Aromatic Molecules*; Wiley: London, 1970.
- (2) Turro, N. J. *Modern Molecular Photochemistry*; Benjamin: Menlo Park, 1978.
- (3) Valeur, B. *Molecular Fluorescence*; Wiley-VCH: Weinheim, 2002.
- (4) Foley, S.; Berberan-Santos, M. N.; Fedorov, A.; Bensasson, R.; Leach, S.; Gigante, B. *Chem. Phys.* **2001**, *263*, 437.
- (5) Texier, I.; Berberan-Santos, M. N.; Fedorov, A.; Brettreich, M.; Schonberger, H.; Hirsch, A.; Leach, S.; Bensasson, R. V. *J. Phys. Chem. A* **2001**, *105*, 10278.

- (6) Rae, M.; Fedorov, A.; Berberan-Santos, M. N. *J. Chem. Phys.* **2003**, *119*, 2223.
- (7) Foote, C. S. *Top. Curr. Chem.* **1994**, *169*, 347.
- (8) Sun, Y. P. In *Molecular and Supramolecular Photochemistry*, Vol. 1, Organic Photochemistry; Ramamurthy, V., Shanze, K. S., Eds.; Marcel Dekker: New York, 1997; pp 325–390.
- (9) Berberan-Santos, M. N.; Garcia, J. M. M. *J. Am. Chem. Soc.* **1996**, *118*, 9391.
- (10) Salazar, F. A.; Fedorov, A.; Berberan-Santos, M. N. *Chem. Phys. Lett.* **1997**, *271*, 361.
- (11) Foley, S.; Berberan-Santos, M. N.; Fedorov, A.; McGarvey, D. J.; Santos, C.; Gigante, B. *J. Phys. Chem. A* **1999**, *103*, 8173.
- (12) Konstantaki, M.; Koudoumas, E.; Couris, S.; Janot, J. M.; Eddaoudi, H.; Deratani, A.; Seta, P.; Leach, S. *Chem. Phys. Lett.* **2000**, *318*, 488.
- (13) Bodunov, E. N.; Berberan-Santos, M. N. *Chem. Phys.* **2004**, *301*, 9.
- (14) Yamamoto, K.; Saunders, M.; Khong, A.; Cross, R. J.; Grayson, M.; Gross, M. L.; Benedetto, A. F.; Weisman, R. B. *J. Am. Chem. Soc.* **1999**, *121*, 1591.
- (15) Bingel, C. *Chem. Ber.* **1993**, *126*, 1957.
- (16) Camps, X.; Hirsch, A. *J. Chem. Soc., Perkin Trans. 1* **1997**, 1595.
- (17) Sun, Y. P.; Riggs, J. E.; Guo, Z.; Rollins, H. W. In *Optical and Electronic Properties of Fullerenes and Fullerene-Based Materials*; Shinar, J., Vardeny, Z. V., Kafafi, Z. H., Eds.; Marcel Dekker: New York, 2000; pp 43–81.
- (18) Berberan-Santos, M. N. *Chem. Phys. Lett.* **1992**, *196*, 220.
- (19) Rikenglaz, M. M.; Rozman, I. M. *Opt. Spectrosc.* **1974**, *36*, 61.